Onset instability of a parametrically excited pendulum array

Weizhong Chen,[1,*] Wengang Lin,[1,2] and Yifei Zhu[1]
[1]*The Key Laboratory of Modern Acoustics and Institute of Acoustics, Nanjing University, Nanjing, 210093, China*
[2]*Ningbo Institute of Education, Ningbo, 315010, China*
(Received 7 June 2006; published 17 January 2007)

In the theoretical framework of the Floquet instability analysis we have investigated the onset instability of the one-dimensional pendulum array, a macroscopic expression of the Frenkel-Kontorova chain, subjected to vertical vibration after the continuum approximation. The Floquet instability calculation shows that the onset instability of the array always responds to the forcing frequency subharmonically. The theoretical predictions of the critical forcing conditions and onset instability waves have been validated by experiments. Good agreement between the theoretical calculations and experimental observations has been achieved for the onset instabilities with both long and short wavelengths.

DOI: 10.1103/PhysRevE.75.016606 PACS number(s): 45.30.+s, 63.20.Ry, 47.20.−k, 63.10.+a

I. INTRODUCTION

The Frenkel-Kontorova (FK) chain [1], a chain of classical particles (atoms) coupled with their nearest neighbors and subjected to a periodic on-site (substrate) potential, has become one of the fundamental and universal models to describe the structure and dynamics of a crystal lattice in the vicinity of the dislocation core in recent years. Many physical phenomena including the adsorbed monolayers [2], Josephson junctions [3], and charge density waves [4], can be investigated in the framework of the FK model. With the rapid development of nanotechnology, some fundamental physical topics, such as heat conduction [5,6] and solid friction [7], have also been studied based on the FK model recently. As a low-dimensional nonlinear physical model, solitary (localized) waves [8,9], chaos [10], and spatiotemporal chaos [11] can appear in the FK chain. Most of the investigations of the FK model are in theory or based on computer simulation. In a macroscopic experiment, the FK chain can be usually expressed as an array of coupled pendulums [12–16]. The pendulum array must be put on a vibrating table to supplement the energy due to the experimental damping. Many nonlinearly localized phenomena, such as kinks [12] and breathers [13], have been observed in this excited pendulum array. However, those localized waves usually do not appear spontaneously. In other words, we may give a suitable initial swing to help the formation of a certain solitary wave. In most cases, with the increase of the excitation the pendulums swing to form a nonlocalized wave without the experimenter's help, which means the onset instability of the excited pendulum array is not a localized wave. The so-called onset instability here denotes the primary envelope wave appearing in the array when it is driven from its stationary state to swinging. As is well known, the onset instability is an important topic in wave theory, such as in hydrodynamic [17,18]. The onset instability of the FK chain relates to many physical backgrounds. We take the heat conduction in crystal [5,6] as an example, if the onset instability of the FK chain is nonlocalized, then we can expect that the temperature distribution is uniform in crystal when the crystal is heated from absolute zero. Furthermore, the properties of the onset instability, such as its frequency and wave number, relate to the thermodynamic behaviors of the crystal closely. However, both the temporal and spacial properties of the onset instability together with the critical forcing conditions remain unknown yet in the excited FK chain theory. In this paper, we will study the onset instability of an array subjected to parametrical excitation in the theoretical framework of a Floquet instability analysis [17]. Then we conduct the corresponding experiments to prove the validity of the theoretical results. In the next section, a linear instability analysis will be developed theoretically for the parametrically forced pendulum array. In Sec. III we will show the main numerical results of the onset instabilities and their corresponding critical forcing conditions. The corresponding experimental validation will be arranged in Sec. IV. Finally, we will present a summary together with a discussion.

II. FLOQUET INSTABILITY ANALYSIS FOR THE FORCED PENDULUM ARRAY

We consider an array of N pendulums coupled to their nearest neighbors and forced vertically. All the pendulums are of same mass m and same pendulum length l. The intrinsic angular frequency of the uncoupled pendulums is $\omega_0 = \sqrt{\frac{g}{l}}$ with g being the acceleration due to gravity. The angle θ_n of the nth pendulum in the array satisfies the dynamics equation

$$ml^2\ddot{\theta}_n + \beta l\dot{\theta}_n - k_2[(\theta_{n+1} - \theta_n) - (\theta_n - \theta_{n-1})] - k_4[(\theta_{n+1} - \theta_n)^3 - (\theta_n - \theta_{n-1})^3] = -ml(g + A_e\omega^2 \cos \omega t)\sin \theta_n, \quad (1)$$

where the overdots denote the derivative with respect to the time t, k_2 and k_4 describe the harmonic and quartic coupling strengths, β is a damping parameter, and A_e and ω are the amplitude and angular frequency of the excitation, respectively. The pendulums at the both ends of the array are fixed,

$$\theta_1 = \theta_N = 0. \quad (2)$$

We are now interested in the primary instability of the array subjected to the vertical vibration, a typical case of

*Corresponding author. Electronic address: wzchen@nju.edu.cn

small-amplitude motion, so that Eq. (1) can be linearized to

$$ml^2\ddot{\theta}_n + \beta l\dot{\theta}_n - k_2[(\theta_{n+1} - \theta_n) - (\theta_n - \theta_{n-1})] = -ml(g + A_e\omega^2 \cos \omega t)\theta_n. \quad (3)$$

Furthermore, the finite differences in Eq. (3) are substituted by their differentials in the long-wavelength approximation [12,13], for the phase-matched mode,

$$(\theta_{n+1} - \theta_n) - (\theta_n - \theta_{n-1}) \approx a^2\theta_{xx}, \quad (4)$$

and for the phase-mismatched mode,

$$(\theta_{n+1} - \theta_n) - (\theta_n - \theta_{n-1}) \approx (-1)^{n+1}(a^2\theta_{xx} + 4\theta), \quad (5)$$

where the subscript x denotes the derivative with respect to the continuum variable x describing the spatial position of the pendulum in the array and a, the lattice constant, is the space between two neighbor pendulums, respectively. The so-called phase-matched and phase-mismatched modes mean that each pendulum has 0 and π phase differences from its immediate neighbors, respectively [12,13]. Under the long-wavelength approximation (4) or (5), N ordinary differential equations (3) for $n=1,2,\ldots,N$ become a partial differential equation in $1+1$ dimensions,

$$\ddot{\theta} + p_\beta\dot{\theta} + (\omega_0^2 + \delta p_d + 2p_l \cos \omega t)\theta - \epsilon p_c\theta_{xx} = 0, \quad (6)$$

where

$$p_\beta = \frac{\beta}{ml}, \quad (7)$$

$$p_c = \frac{a^2k_2}{ml^2}, \quad (8)$$

$$p_l = \frac{A_e\omega^2}{2l}, \quad (9)$$

and

$$p_d = \frac{4k_2}{ml^2}, \quad (10)$$

with $\delta=0$, $\epsilon=1$ for the phase-matched mode and $\delta=1$, $\epsilon=-1$ for the phase-mismatched mode, respectively.

We now investigate the onset instability for this excited pendulum array in the theoretical framework of a Floquet instability analysis [17]. Considering the boundary condition (2), we expand the angle $\theta(x,t)$ into the following form:

$$\theta(x,t) = e^{(s+i\alpha\omega)t} \sin kx \sum_{n=-\infty}^{\infty} a_n e^{in\omega t}, \quad (11)$$

where a_n $(n=\pm1,\pm2,\ldots)$ are expanding coefficients and $(s+i\alpha\omega)$ is a Floquet exponent with s and α being real. A positive growth factor $s>0$ corresponds to the growth of the instability and $s<0$ to the suppression of the instability. The values $\alpha=0$ and $\alpha=\frac{1}{2}$ of the imaginary part of the exponent correspond to the harmonic and subharmonic responses to the forcing frequency, respectively. The wave number k in Eq. (11) is determined by the boundary conditions (2)—that is,

$$\theta(x,t)|_{x=0,L} = 0, \quad (12)$$

where $L=Na$. Obviously the wave number has to be discretized to satisfy the stationary ends, $k=k_j=\frac{j\pi}{L}$ $(j=1,2,\ldots)$. For the case of the large N, of course, k_j regenerates to the continuum. Substituting Eq. (11) into Eq. (6), we obtain a recursion relation for expanding coefficients a_n $(n=0,\pm1,\pm2,\ldots)$,

$$qa_{n-1} + (\epsilon k_j^2 + p_n)a_n + qa_{n+1} = 0, \quad (13)$$

where

$$p_n = \frac{1}{p_c}\{[s + i(\alpha+n)\omega]^2 + p_\beta[s + i(\alpha+n)\omega] + \omega_0^2 + \delta p_d\} \quad (14)$$

and

$$q = \frac{ml\omega^2}{2a^2k_2}A_e. \quad (15)$$

Furthermore, Eq. (13) can be rewritten as

$$\sum_{n=-\infty}^{\infty} (\mathcal{M}_{l,n} + \mathcal{N}_{l,n})a_n = 0 \quad (l=0,\pm1,\pm2,\ldots), \quad (16)$$

where

$$\mathcal{M}_{l,n} = \delta_{l,n}(\epsilon k_j^2 + p_n) \quad (l,n=0,\pm1,\pm2,\ldots), \quad (17)$$

$$\mathcal{N}_{l,n} = (\delta_{l,n-1} + \delta_{l,n+1})q \quad (l,n=0,\pm1,\pm2,\ldots), \quad (18)$$

where $\delta_{n,l}$ is a Kronecker delta function. The nontrivial condition of the homogenous algebra equation (16),

$$\det(\mathcal{M} + \mathcal{N}) = 0, \quad (19)$$

will give us the relation between the growth factor s and driving parameters, the acceleration amplitude $a_e=A_e\omega^2$, and the angular frequency ω together with the temporal response mode α and spatial distribution k_j. Usually in the framework of a linear analysis of the instability we can distinguish the array between the rest and swing by computing the growth factor s for each spatial mode k_j, $(j=1,2,\ldots)$ and temporal mode α under the excitation of $a_e \cos \omega t$. We can also calculate the threshold acceleration amplitude $a_{th}(k_j)$ over which the array may start to swing from rest and to form an envelop wave with wave number k_j by setting $s=0$ in Eq. (19).

III. CRITICAL ACCELERATION AND ONSET WAVE FORM

Before the numerical calculation, it is necessary to truncate the infinity order matrices $\mathcal{M}$ and $\mathcal{N}$ to a finite order in Eq. (19). In other words, we would truncate the summation in Eq. (16) from $(-\infty,\infty)$ to $[-N_{trun},N_{trun}]$ with N_{trun} being an integer. For the truncating number N_{trun} the matrices $\mathcal{M}$ and $\mathcal{N}$ are of order $2N_{trun}$ if $\alpha=1/2$ or $2N_{trun}+1$ if $\alpha=0$. Although the approximation due to the truncation is unavoidable, the calculating precision can always be reached by enlarging N_{trun}. Furthermore, the truncating approximation usu-

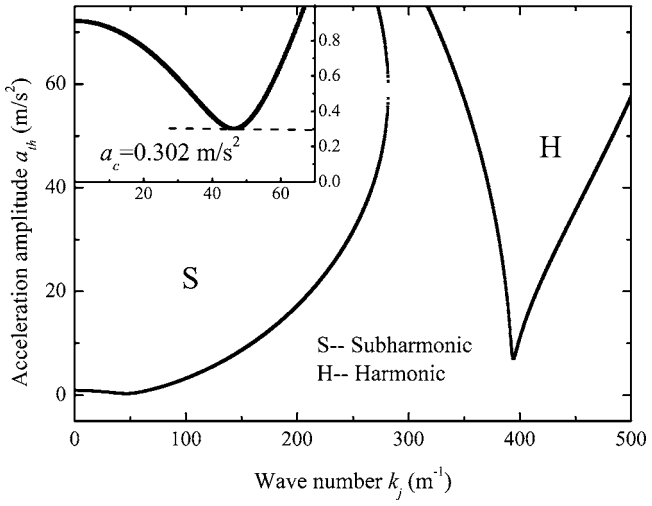

FIG. 1. Stability boundary against the phase-matched instability. Below the curves the pendulums remain at rest. Over the curves the array starts to oscillate in the phase-matched mode subharmonically (S) or harmonically (H). The parameters are $\omega/2\pi=3.60$ Hz, $k_2=1.21\times10^{-4}$ J, and $\beta=4.0\times10^{-5}$ kg m/s, respectively.

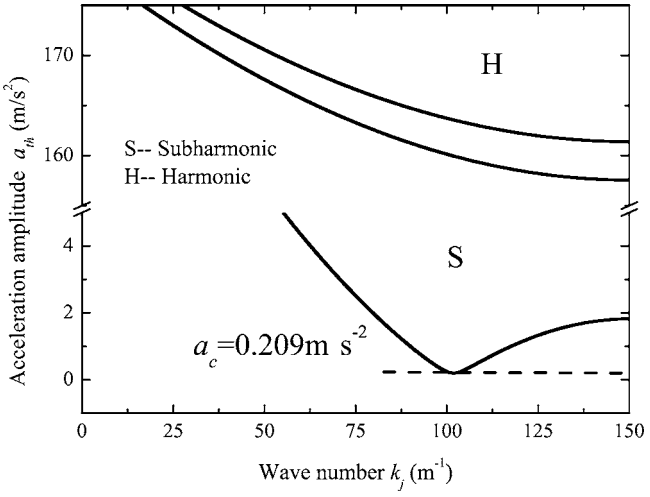

FIG. 2. Stability boundary against the phase-mismatched instability. Below the curve the pendulums remain at rest. Over the curves the array starts to oscillate in the phase-mismatched mode subharmonically (S) and harmonically (H). The parameters are $\omega/2\pi=4.00$ Hz, $k_2=2.30\times10^{-4}$ J, and $\beta=2.40\times10^{-5}$ kg m/s, respectively.

ally possesses a good convergence [17,18]. In fact, the expanding coefficients a_n, $(n=-N_{trun},-N_{trun}+1,\ldots,N_{trun}-1,N_{trun})$ are not independent due to the reality of the $\theta(x,t)$ in Eq. (11)—that is,

$$a_{-n}=a_n^* \quad (\text{if } \alpha=0) \tag{20}$$

or

$$a_{-n}=a_{n-1}^* \quad (\text{if } \alpha=1/2), \tag{21}$$

where * denotes the complex conjugate.

Taking $N_{trun}=20$ we calculated the threshold acceleration amplitudes a_{th} for different wave modes k_j $(j=1,2,\ldots)$. The calculated result is plotted in Figs. 1 and 2 for the phase-matched mode and the phase-mismatched mode, respectively. In these figures the stability curves $a_{th}(k_j)$ present the usual resonance tongue structure [17–19]. The harmonic and subharmonic tongues, labeled by H and S in Figs. 1 and 2, indicate regions where the pendulums become unstable, oscillating at an integral multiple frequency $\omega,2\omega,3\omega,\ldots$ or an odd half-multiple frequency $\omega/2,3\omega/2,5\omega/2,\ldots$, respectively. The tongues at higher wave number k_j correspond to instabilities with shorter wavelengths and higher oscillation frequencies. Our calculation, of course, is limited to the case with lower wave number due to the long-wavelength approximation (4) or (5). The primary or onset instability wave takes place at the lowest tangent point of tongues (see the inset of Fig. 1). In both phase-matched and phase-mismatched modes the onset instability waves do not respond to the forcing frequencies harmonically. The pendulums in the array always start to oscillate from the rest at the half forcing frequency when the exciting acceleration amplitude increases gradually (see Figs. 1 and 2). The critical acceleration amplitudes are $a_c=0.302$ m/s^2 and $a_c=0.209$ m/s^2 for phase-matched and phase-mismatched modes, respectively. It is noticeable that the onset wave in the phase-mismatched mode needs lower forcing energy than that in the phase-matched mode.

IV. EXPERIMENTAL VALIDATION

The experimental apparatus used here was similar to those in Ref. [16] (see Fig. 3). The experimental array consisted of $N=47$ pendulums supported by a rod, with equal spacing $a=20.0$ mm from each other. The pendulum mass and length were $m=3.0$ g and $l=82.0$ mm, respectively. Every pendulum was coupled with its nearest neighbor by fixing overlapping points of their V-type pendulum strings [12,13,16]. The deviations in mass and length were less than 0.003 g and 0.1 mm in our experimental array, respectively.

The array was attached to a vertically vibrating table driven by an exciter (Brüel & Kjær 4812). The driven sinu-

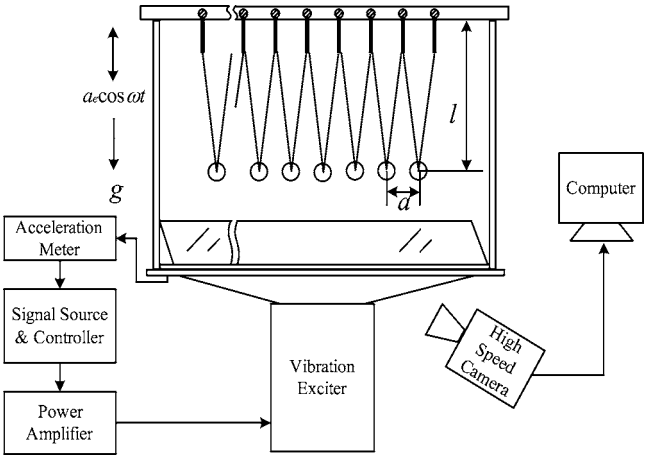

FIG. 3. Schematic of the experimental apparatus.

TABLE I. Comparison between experimental and theoretical results.

	f (Hz)	a_c (m s^{-2})	k_c (m^{-1})	Mode
Expt.	3.600	0.309	43.4	Matched
Theor.	3.600	0.302	38.6	Matched
Expt.	4.000	0.228	133.7	Mismatched
Theor.	4.000	0.209	114.4	Mismatched

soidal voltage was generated by an exciter controller (Brüel & Kjær 1050), then amplified by a power amplifier (Brüel & Kjær 2707). An accelerometer fixed on the table provided a feedback signal to the exciter controller, which holds the vibration of the exciter accurately. The resolutions of the frequency and acceleration were 1 mHz and 0.001 m/s^2 in our experimental system, respectively.

A digital image workstation equipped with a high-speed charge coupled device (CCD) was used to acquire the distribution of the array and its evolution. The images of the pendulums were reflected by a mirror with an inclination angle of 45° located beneath the array and then captured by the CCD. The locations of the pendulums were recognized from the background by an image-processing code and then converted to angular displacements θ_n $(n=1,\ldots,N)$. We could obtain the wave number of the instability by an fast Fourier transform (FFT) calculating according to θ_n $(n=1,2,\ldots,N)$. We could also compute the temporal response mode of the instability by acquiring a time series of a certain pendulum—e.g., the pendulum at center $(n=24)$.

In experiment, we adjusted the forcing frequency $f=\omega/2\pi$ to that we desire to do, such as 3.600 Hz in Fig. 1, then increased the acceleration amplitude gradually until the pendulums started to swing. For each acceleration amplitude we kept the excitation for 10 min to judge whether the pendulums were stable or unstable. By this way we can get a critical acceleration amplitude a_c together with all information about the corresponding onset instability wave at this forcing frequency f. The experimental observations supported the theoretical predictions that the onset instabilities responded to the forcing frequency subharmonically in both phase-matched and phase-mismatched modes. The experimental measurements for a_c and k_c quite well agreed with those calculated in Figs. 1 and 2 (see Table I).

In fact, we changed forcing frequency f from 3.500 Hz to 4.200 Hz by a step 0.050 Hz and repeated the measurement above. In Fig. 4 we show the experimental measurement results. The critical acceleration amplitude a_c has a complicated relation to the forcing frequency f. There is a frequency well in which a low a_c can force the array to swing. On the well wall ($f=3.500$ or 4.200 Hz), however, we have to use a very large a_c to excite a wave. The well is located in the frequency band slightly higher than the double intrinsic frequency $f_0=\omega_0/\pi$ (see a downward arrow in Fig. 4). There is a valley at $f=4.100$ Hz in the bottom of the well at which the critical acceleration amplitude a_c reaches its minimum 0.192 m/s^2. It is understandable that the well is a result of the parametric resonance. As the forcing frequency increases, of course, the wavelength of the onset instability will become shorter and shorter (see Fig. 5). As a result, the wave mode changes from the phase-matched mode to phase-mismatched mode gradually.

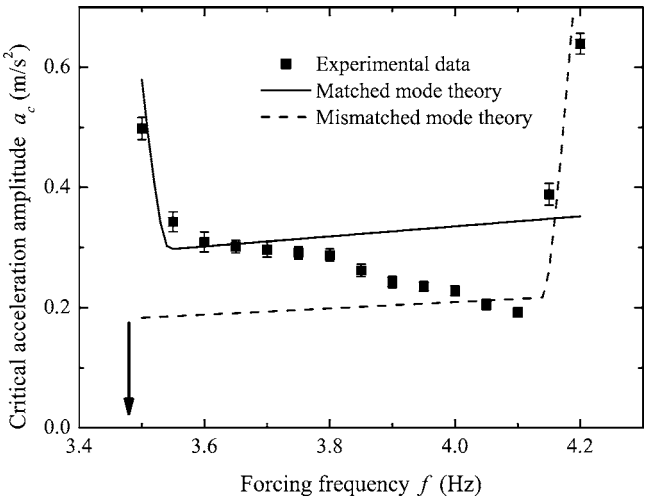

FIG. 4. The onset acceleration amplitude under different forcing frequencies. The solid curve is for the phase-matched mode, the dashed one for the phase-mismatched mode. The arrow points to the double intrinsic frequency f_0 of the pendulum.

In theory, for a given frequency f we can obtain a stability boundary like Fig. 1 or 2 by calculating Eq. (19), then get the critical acceleration amplitude a_c together with the corresponding onset instability wave number k_c. These theoretical computations have been plotted by solid curve for the phase-matched mode and dashed curve for the phase-mismatched mode in both Figs. 4 and 5. It is easy to see in Figs. 4 and 5 that the solid and dashed curves agree with the experimental data well in the lower- and higher-frequency bands, corresponding to longer- and shorter-wavelength regions, respectively. In both of them, however, the data deviate in the medium-frequency band corresponding to the medium-wavelength region. As mentioned above the wave with long

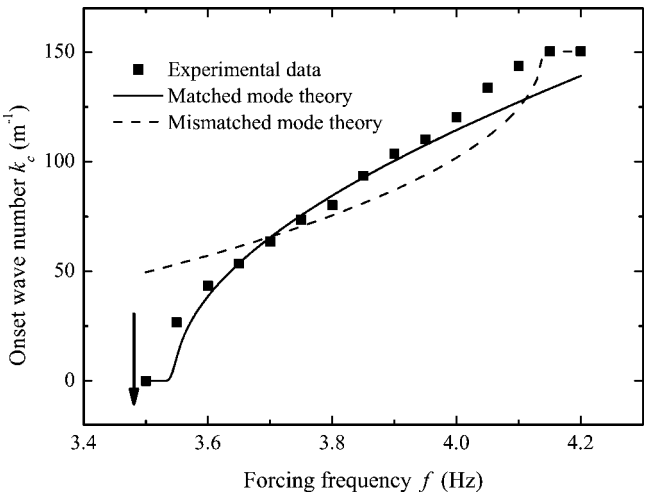

FIG. 5. The onset wave number under different forcing frequencies. The solid curve is for the phase-matched mode and the dashed one for the phase-mismatched mode. The arrow points to the double intrinsic frequency f_0 of the pendulum.

wavelength in the phase-matched mode is a real long wave, while that in the phase-mismatched mode corresponds a short wave in fact. Therefore, the instability analysis here can well explain the observations of the onset instabilities with both long and short wavelengthes, and may deviate from the data in medium-wavelength region.

V. SUMMARY AND DISCUSSION

In the theoretical framework of the Floquet instability analysis we have investigated the onset instability of the one-dimensional pendulum array subjected to vertical vibration. The linear instability analysis developed by Kumar [17] has been used to calculate the critical acceleration amplitude and corresponding onset instability mode. In the calculation the long-wavelength approximation has been employed to transform the discrete array to a continuum system. The theoretical calculation can not only precisely compute the onset instability with long wavelength, but also predict that with short wavelength because both phase-matched and phase-mismatched modes have been considered. The calculation shows that the onset instability of the array always responds to the forcing frequency subharmonically. And the onset pattern is a sinusoidal wave with a single wave number, which is consistent with experimental observations [13,16]. In experiment, as the forcing amplitude is small the pendulums always swing to form a sinusoidal wave, instead of a solitary wave. The nonlinear interaction makes the envelop wave localized when the forcing amplitude is large enough. There is a frequency well in the energy absorption of the array from the external excitation. The critical forcing conditions together with the onset instability waves have been checked by our experiments. Good agreement between the theoretical calculations and experimental observations has been achieved for the onset instability with both long wavelength and short wavelength. A small deviation from the experimental data has also found when the onset instability is in the medium-wavelength band because the investigation here is limited by the continuum-wave approximation.

ACKNOWLEDGMENTS

This work was supported in part by National Nature Science Foundation of China (Grant Nos. 10374050 and 10434070) and the Key Project of Chinese Ministry of Education (No. 103078).

[1] O. M. Braun and Y. S. Kivshar, Phys. Rep. **306**, 1 (1998).
[2] O. M. Braun *et al.*, Phys. Rev. Lett. **78**, 1295 (1997).
[3] R. S. Newrock, C. J. Lobb, U. Geigenmuller, and M. Octavio, Solid State Phys. **54**, 263 (2000).
[4] J. B. Sokoloff, J. E. Sacco, and J. F. Weisz, Phys. Rev. Lett. **41**, 1561 (1978).
[5] B. W. Li, J. H. Lan, and L. Wang, Phys. Rev. Lett. **95**, 104302 (2005).
[6] E. Pereira and R. Falcao, Phys. Rev. Lett. **96**, 100601 (2006).
[7] O. M. Braun, A. Vanossi, and E. Tosatti, Phys. Rev. Lett. **95**, 026102 (2005).
[8] L. L. Bonilla and B. A. Malomed, Phys. Rev. B **43**, 11539 (1991).
[9] J. L. Marin, F. Falo, P. J. Martinez, and L. M. Floria, Phys. Rev. E **63**, 066603 (2001).
[10] P. J. Martinez and R. Chacon, Phys. Rev. Lett. **93**, 237006 (2004).
[11] R. Chacon, Phys. Rev. Lett. **86**, 1737 (2001).
[12] B. Denardo *et al.*, Phys. Rev. Lett. **68**, 1730 (1992).
[13] W. Z. Chen, Phys. Rev. B **49**, 15063 (1994).
[14] N. V. Alexeeva, I. V. Barashenkov, and G. P. Tsironis, Phys. Rev. Lett. **84**, 3053 (2000).
[15] W. Z. Chen, B. B. Hu, and H. Zhang, Phys. Rev. B **65**, 134302 (2002).
[16] W. Z. Chen, Y. F. Zhu, and L. Lu, Phys. Rev. B **67**, 184301 (2003).
[17] K. Kumar, Proc. R. Soc. London, Ser. A **452**, 1113 (1996).
[18] W. Z. Chen and R. J. Wei, Phys. Rev. E **57**, 4350 (1998).
[19] C. Huepe, Y. Ding, P. Umbanhowar, and M. Silber, Phys. Rev. E **73**, 016310 (2006).